EFFECT OF VARIABILITY OF MECHANICAL PARAMETERS ON THE DEFORMATION BEHAVIOUR AND FAILURE OF FIBRE REINFORCED PLASTIC MATERIALS

László Kovács[1], Gábor Romhány PhD[2]

[1]eCon Engineering Ltd, 1116 Budapest Kondorosi út 3. Floor IV, Hungary
Email: laszlo.kovacs@econengineering.com, Web Page: http://www.econengineering.com
[2]Department of Polymer Engineering, Faculty of Mechanical Engineering, Budapest University of Technology and Economics, 1111, Budapest, Műegyetem rkp. 3., T block, Floor III, Hungary
Email: romhany@pt.bme.hu, Web Page: http://www.pt.bme.hu

Keywords: scatter in material properties, imperfections, stress analysis, safety factor, probability to failure

Abstract

The accurate predictions of the mechanical performance of composite structures has a major importance that does depend on the uncertainty levels of the underlying material models and on the implications of manufacturing process and defects.
The presented work introduces a Monte-Carlo sampling based approach that aims to model the effect of the variability in terms of stiffness and strength of the baseline composite material on the behavior of a slender structure such as a composite bicycle frame.
As part of this work an inherent probability distribution was assumed for the stiffness parameters of the constitutive materials of an E-Glass/Epoxy composite system. From this, the probability distribution of the baseline composite ply was estimated and with an appropriate sampling method it was applied on a Finite Element model of a slender bicycle frame structure including a resin pocket as a very low fiber content zone.
The results show that the scatter in material data can lead to significant variation in the level of utilization of the assessed structure. In addition, the presence of a resin pocket can create unexpected critical locations therefore ignoring these imperfections in the design phase can lead to unsafe products.

1. Introduction

Polymer composite parts are light, stiff and can be very durable due to the possibility to design the ply structure so that it fits for purpose. However, nowadays such high performance composite components can only be safely used in exclusive applications and narrow industry segments such as aerospace industry, sport and race car industry etc. Partly the reason for this is the relatively high uncertainty levels including the underlying material models (deformation as well as static failure, damage tolerance and fatigue) and the implications of manufacturing process and defects on the mechanical performance. Present work focuses on the extensive variation of the material properties that is one aspect making the design of such parts complicated.
In practice composite structures are modelled in FEM environment on a ply-by-ply basis. The plies are homogenized meaning that the local inhomogeneity of the fiber-resin system is neglected treating one layer as a homogenous material with a certain extent of anisotropy.
From the ply behavior the stiffness and deformation of the whole laminate can be forecast by using an appropriate plate theory (e.g. Kirchhoff plate theory [1] [2], Reissner-Mindlin theory [1] etc.).
It follows from above that in the deformation and failure modelling process of a laminated plate the ply-specific engineering constants (moduli and Poisson's ratios) as well as strength (stress limits, failure envelope constants etc.) parameters are basic inputs therefore the accurate evaluation of those is essential.

However, unlike metals in composite industry the suppliers can only guarantee the material properties of the constituents (fiber and resin) since the composite material is actually made by the manufacturer together with the final product. Therefore ply specific properties cannot be obtained by suppliers, it shall be evaluated as a function of the ply stackup, manufacturing process parameters etc.
In industrial practice the necessary ply specific material parameters are evaluated from standard mechanical tests. One big advantage of mechanical experiments is that one can gain information about the scatter in the measured parameters. Knowing the scatter can feed a new approach represented by this work where each parameter determining the stiffness and strength of a ply is rather a probabilistic variable than a single number. This probabilistic variable can be characterized by a Probability Density Function (PDF) and a Cumulative Distribution Function (CDF) telling the probability of the parameter to take a given value.

2. Input data for constituents

The input to the investigation was the set of stiffness parameters for the fiber and the resin assumed to build the composite in question. E-Glass unidirectional (UD) fiber reinforcement structure was assumed for one ply embedded in Epoxy resin. The input mean engineering constants were taken from literature [5]. The standard deviation of those relative to the mean (Relative Standard Deviation - RSD) were estimated based on industrial experience. These inputs are collected in Table 1.

Table 1. Stiffness constants of the constituents used in the analyses.

Constituent	Mean E (GPa)	Mean ν	RSD of E (%)	RSD of ν (%)
E-Glass Fiber	72	0.1	30	10
Epoxy Resin	3	0.3	10	10

Assuming isotropic material, the shear modulus of the constituents (G) was analytically calculated from the inputs above with the formula:

$$G = \frac{E}{2\cdot(1+\nu)}\,. \tag{1}$$

3. Methodology

3.1. Generation of sampled laminate stiffness data

In present work the PDF and CDF of the stiffness parameters was established by a Monte-Carlo sampling method where using an inherent CDF of the fiber and resin stiffness parameters as inputs the composite layer characteristics were calculated repeatedly with the use of Voigt-Reuss [3] and Halpin-Tsai [4] based RoM. Normal (Gaussian) distribution was assumed for the fiber and matrix material that has the mean and the RSD as two independent parameters. The Voigt-Reuss equations were implemented to evaluate the in-plane stiffness constants [3].
After a large number of simulations (10^6) it was possible to generate empirical PDF and CDF for the engineering constants of the ply. Two sets of CDFs were created for a low (10%) and a high (60%) fiber volume fraction (V_f) cases, representing a resin pocket as a manufacturing defect and the ideal composite respectively. For simplification reasons these empirical CDFs were also treated as Gaussian functions and the parameters for the CDF of each stiffness constant were fitted with least squared method. It is worth to mention that for E_{22}, G_{12} and the out-of-plane stiffness constants this assumption is not fully correct, however the quality of the fit was deemed to be acceptable. Since the Voigt equation is fully linear, the E_{11} and ν_{12} of the ply turned out to follow a normal distribution with the following parameters (denoted as X_{mean} and X_{STDEV}) where the index "i" refers to one calculation with the "i-th" sampled inputs:

$$X_{mean} = \frac{\sum_{i=1}^{10^6} X_i}{10^6}, \quad (2)$$

$$X_{STDEV} = \sqrt{\frac{\sum_{i=1}^{10^6}[(X_i - X_{mean})^2]}{10^6}}. \quad (3)$$

These distribution functions were then used to sample 100 sets of material constants with the Monte-Carlo method. The sampled sets were input material data cards to 100 independent FE calculations of a slender composite frame of a fictitious bicycle with and without the presence of resin pocket in a pre-selected critical area.

3.2 Estimation of failure model constants

In order to assess the FE stress results an appropriate failure model was selected for post-processing. In order to be keep the model relatively simple but still account for the interaction of the individual stress components within a ply the two-dimensional Tsai-Wu criterion was chosen for this purpose. The parameters of that had to be estimated separately for the baseline composite material and for the resin rich area. For the baseline E-Glass/Epoxy system the strength values were taken from literature [5] and the dimensionless Tsai-Wu stress interaction constant (denoted as F_{12}*) was assumed to be -0.5 as a typical number for such composite systems as per [6]. For the resin rich area conservatively the pure resin strength was taken from [5] and assuming it to be isotropic the von Mises yield criterion was implemented here as the failure envelope. In this case all normal strength components are identical (as being the "yield stress") and the shear strength follows from the pure shear case of the Mises equation:

$$S_{12} = \frac{S_{11}}{\sqrt{3}}, \quad (4)$$

where S_{12} denotes shear limit and S_{11} stands for yield strength in pure tension.
The von Mises yield criterion can be expressed with the Tsai-Wu equation as well since that is a more generalized formulation giving F_{12}*=-0.5. The Tsai-Wu parameters used are collected in Table 2. The numbers in the indices correspond to the relevant stress component, "t" refers to tension, "c" refers to compression.

Table 2. Lamina Tsai-Wu failure parameters used in the analyses.

	$S_{11\text{-t}}$ (MPa)	$S_{11\text{-c}}$ (MPa)	$S_{22\text{-t}}$ (MPa)	$S_{22\text{-c}}$ (MPa)	S_{12} (MPa)	F_{12}*
Baseline composite	1020	-490	8	-78	23	-0.5
Resin pocket	64	-64	64	-64	37	-0.5

3.3. Description of the Finite Element Model used for sensitivity analysis

To demonstrate the sensitivity to input material data, a slender composite structure was chosen to analyze. A slender body produces larger deformations and thus, stresses that can magnify the effect of scatter in material data. As an ideal candidate a fictitious bicycle frame was created consisting of composite monolithic and sandwich sections. The frame was simulated with layered shell elements and run with the implicit solver of ANSYS 18.2. In ANSYS this layered shell element type is called Shell 181 with a linear shape function associated.
The number of triangular elements were attempted to be minimum during meshing in order to produce a structured mesh as much as possible. The used mesh quality limits ensured acceptable quality of the computed stresses. Since the same calculation was repeated 100 times with the sampled material

parameters the calculation time was a key parameter. This is the reason why keeping the total number of elements low was important. As a result of this, the meshed frame contained app. 6000 shell elements. The modelled section of the bicycle along with its context and dimensions is highlighted in (Fig. 1.).
Some simplifications were made on the model. In practice a composite bicycle frame is manufactured via joining the individual parts (main body, front tube, forks, rear tube etc.) with adhesives that usually are stiffer than the baseline material itself. These stiff zones at the transition between individual building parts were not included.
The forks and the main body was assumed to be a sandwich body while all tubular sections were specified to be simple monolithic plates not filled with core. Each monolithic laminate was defined to have 8 layers of the E-Glass/Epoxy system detailed earlier forming a quadroaxial $[0/45/-45/90]_s$ multidirectional laminate (MD) symmetric to the middle plane. In case of sandwich structures the two symmetric halves of this structure were separated by an isotropic homogeneous PET core with elastic constants from [7]. The composite layup definition was performed in ANSYS Composite PrePost (ACP) software where the fiber orientation was set according to the presumed UD textile preparation process, however, for a quadroaxial laminate the global behavior is quasi isotropic, thus, the fiber orientations did not affect the results.
The loads and boundary conditions (BC) are highlighted in (Fig. 1). Green arrows represent constrained movements modelling the effect of wheel-road contact and the red ones the forces triggered when the cyclist attempts to accelerate by placing his whole body weight on one pedal while grabbing the handle based on [8]. All loads and BCs were introduced to the frame with the aid of rigid constrains (CERIG).

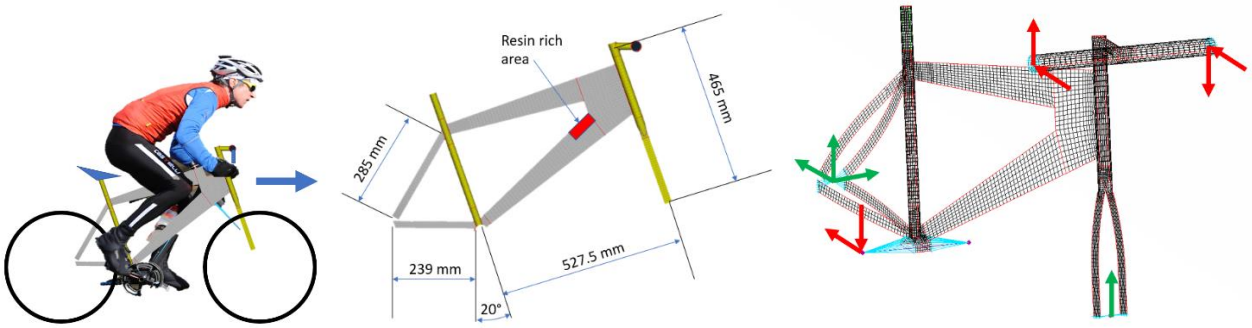

Figure 1. The modelled geometry of a bicycle frame with the relevant dimensions and loads/BCs.

Two individual series of runs were conducted, one with ideal composite structure and another with a resin rich area type defect as shown in (Fig. 1). For the element set representing the resin rich area (resin pocket) the ply-specific material constants derived for V_f of 10% were used.

4. Results

4.1. Derived Cumulative Distribution Functions for ply-specific material constants

The parameters of the final ply-specific material constant distribution functions are collected in Table 3. The diagrams in (Fig. 2) and (Fig. 3) show the empirical (continuous) and fitted (symbols) distribution functions for E_{11} and G_{12} for the two selected fiber content values (10% and 60%). The two theoretical limits are also shown: the black dashed line corresponds to the CDF of the resin, the red one is the CDF for the fiber.

Table 3. Material parameters of the analyzed composite ply derived with Monte-Carlo method.

V_f (%)	Mean E_{11} (GPa)	RSD of E_{11} (%)	Mean ν_{12}	RSD of ν_{12} (%)	Mean E_{22} (GPa)	RSD of E_{22} (%)	Mean G_{12} (GPa)	RSD of G_{12} (%)	Mean ν_{23}	Mean G_{23} (GPa)
10	9.9	22	0.28	9.64	3.32	9.95	1.27	10	0.531	1.08
60	44.4	29.1	0.18	7.45	7.1	10	2.72	8	0.669	2.1

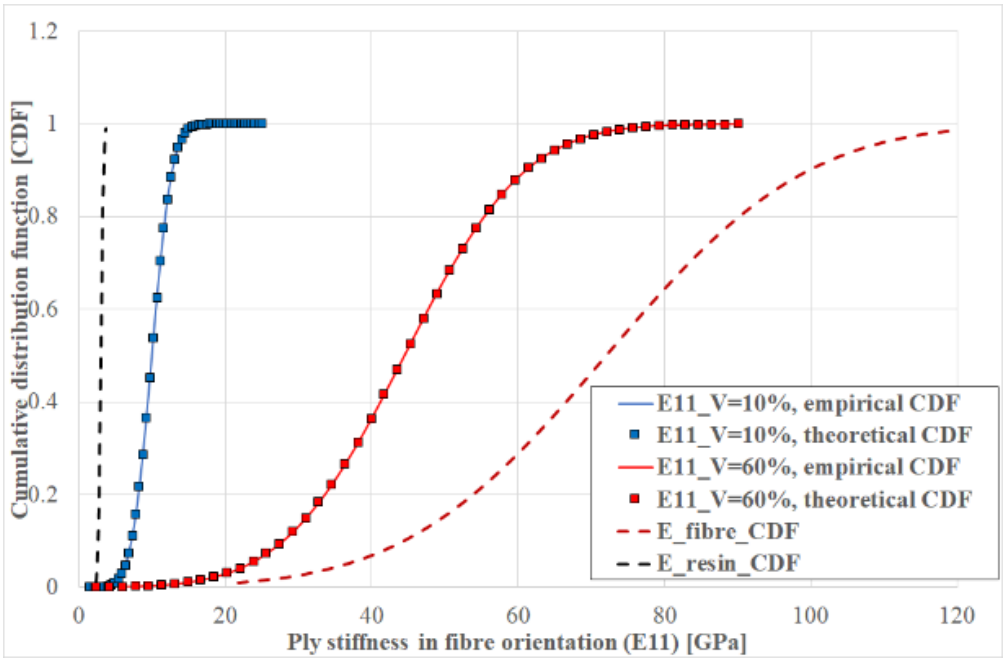

Figure 2. CDFs for E_{11} generated for the analyzed composite ply for V_f=10% and 60%.

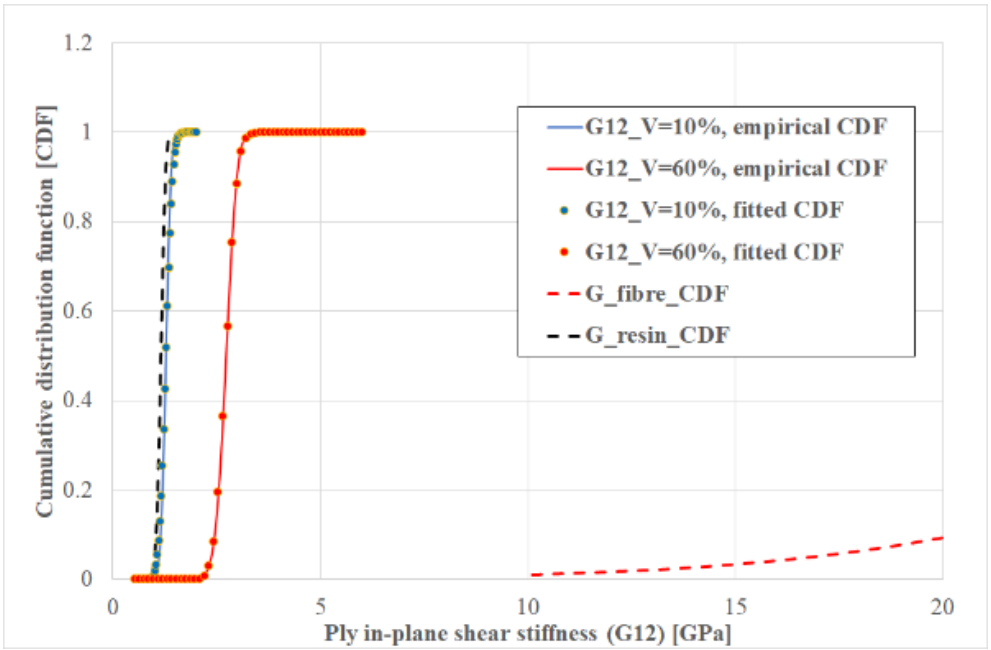

Figure 3. CDFs for G_{12} generated for the analyzed composite ply for V_f=10% and 60%.

4.2. Results of the FE analysis series

A typical deformation result for the assessed bicycle frame is highlighted in (Fig. 4). The main load appeared to be a twist of the frame. ACP was exploited to automatically assess all layers of all finite elements with the relevant 2D Tsai-Wu criterion. Based on this, the zone shown in (Fig. 4) was chosen for further statistical assessment as it exhibited a high level of utilization. The elements colored in red in the picture on the right hand side indicate the Tsai-Wu Inverse Reserve Factor (IRF) > 1.

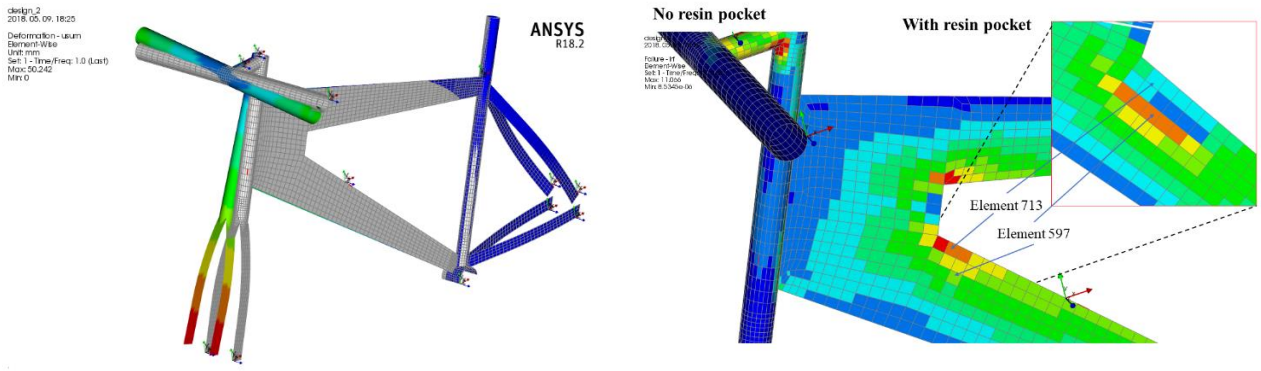

Figure 4. Deformed shape and the selected highly utilized area of the analyzed model.

Elements 597 and 713 were selected for further investigation involving the statistical assessment of the 100 FE results. Element 713 is a critical location when no resin pocket exists. After adding a resin pocket to the zone highlighted in (Fig. 1) the significantly reduced stiffness in that zone pushes down the stresses and in the boundary region of the resin rich area a new critical zone appears represented by element 597 as shown in (Fig. 4). For the aforementioned two elements the Tsai-Wu IRFs were collected from the runs and the variation as a result of the scatter in input material parameters was visualized via density histograms. For all runs both with and without resin pocket the top section of layer 6 appeared to be the critical which is the ply adjacent to the sandwich core on the pulled side of the layup. These histograms are highlighted in (Fig. 4). The red and blue solid lines represent Element 597 without and with resin pocket present respectively. Similarly, the green and yellow solid lines show the IRF variation of Element 713 for the aforementioned two scenarios.

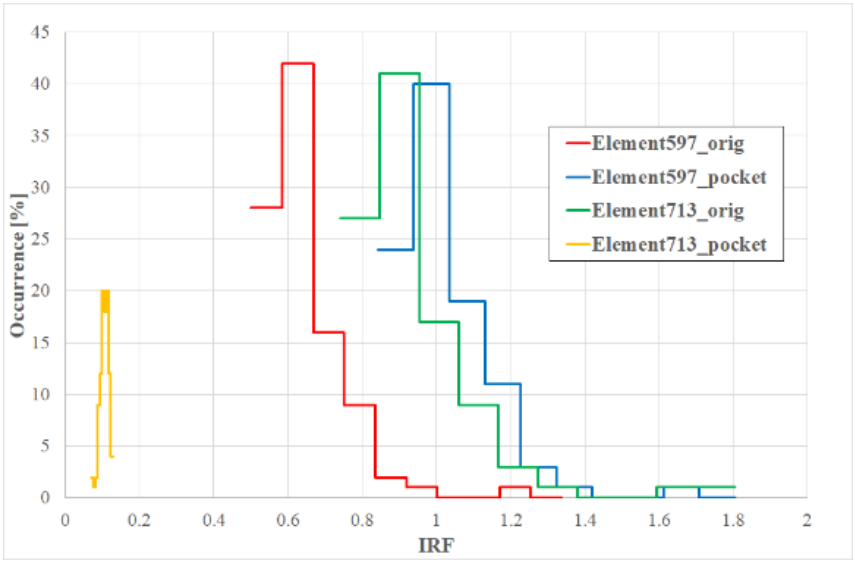

Figure 5. Density histograms of IRF at the locations of interest.

Risk of failure was computed from the statistical processing of the results of individual FE calculations. This gave a rise of the risk from 2% to 49% for Element 597 while for Element 713 it dropped from 23% to practically zero. The range within which the IRFs can be found with 95% confidence (normalized by the weighted average value) became narrower (35% → 27% for Element 597 and 42% → 28% for Element 713) that somewhat counteracts the unwanted trend of increasing risk to failure.
The empirical PDF of vertical displacement of the handlebar end was also generated for both scenarios since that location exhibited the largest movements. It is shown in (Fig. 6). It follows from the diagrams that the presence of resin rich area does not affect the deformation of a location being relatively remote from the local manufacturing imperfection. It is also clear from (Fig. 6) that the distribution of the displacement is not symmetrical although the input composite constituent property CDFs followed a symmetrical Gaussian distribution.

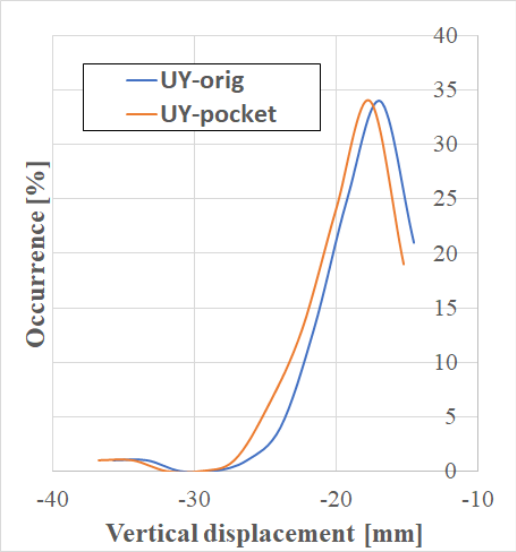

Figure 6. Empirical PDFs of handlebar vertical displacement with and without resin pocket.

5. Conclusions

Present case study proved that the variation in the material properties of the constituents of a composite system can lead to an extent of uncertainty of computed stresses that is not tolerable. The Monte-Carlo based method introduced in this work also envisages a new way of thinking in the design and assessment of composite structures where the variation in material data is considered and the performance of a structure can be evaluated corresponding to a certain probability of survival level. This probabilistics based approach can also validate safety factors used in practice and can also produce part-specific safety factors representing the scatter in the computed stresses, and thus levels of utilizations.

Acknowledgments

I would like to offer thanks to the National Research, Development and Innovation Fund (NKFIA) of Hungary for the financial support of this study being part of a research and development (R&D) project called NVKP16-1-2016-0046, launched within the scope of the National Competitiveness and Excellence Programme (NCEP).

References

[1] N. Reddy J. *Mechanics of Laminated Composite Plates and Shells Theory and Analysis.* CRC Press, Boca Raton, 2004.
[2] https://www.colorado.edu/engineering/CAS/courses.d/AFEM.d/AFEM.Ch20.d/AFEM.Ch20.pdf [Online].
[3] L. D. Kollár, D. S. Springer. *Mechanics of Composite Structures*. Cambridge University Press, 2003.
[4] J. C. Halpin, J. L. Kardos. The Halpin-Tsai Equations: A Review. *Polymer Engineering and Science*, 16: 344-352 , 1976.
[5] S. T. Peters. *Handbook of Composites.* Springer-science+business media, B.V., 1998.
[6] Shuguang Li, Elena Sitnikova, Yuning Liang, Abdul-Salam Kaddour. The Tsai-Wu failure criterion rationalised in the context of UD composites. *Composites: Part A*, 102: 207-217, 2017.
[7] Airex Baltek Banova. Airex® T90 Data Sheet, 2012.
[8] Derek Covill, Steven Begg, Eddy Elton, Mark Milne, Richard Morris, Tim Katz. Parametric finite element analysis of bicycle frame geometries. *Procedia Engineering*, 72: 441-446, 2014.